TU Delft

Delft University of Technology

Document Version
Final published version

Licence
CC BY

Citation (APA)
Boshoven, J., Vigier, J. F., Pöml, P., Ndiaye, A., Morel, B., Konings, R. J. M., Popa, K., & Cologna, M. (2025). Low-temperature sintering of (U,Pu)O2 MOX in mild oxidative conditions. *Journal of Nuclear Materials*, *610*, Article 155800. https://doi.org/10.1016/j.jnucmat.2025.155800

Important note
To cite this publication, please use the final published version (if applicable).
Please check the document version above.

Copyright
In case the licence states “Dutch Copyright Act (Article 25fa)”, this publication was made available Green Open Access via the TU Delft Institutional Repository pursuant to Dutch Copyright Act (Article 25fa, the Taverne amendment). This provision does not affect copyright ownership.
Unless copyright is transferred by contract or statute, it remains with the copyright holder.

Sharing and reuse
Other than for strictly personal use, it is not permitted to download, forward or distribute the text or part of it, without the consent of the author(s) and/or copyright holder(s), unless the work is under an open content license such as Creative Commons.

Takedown policy
Please contact us and provide details if you believe this document breaches copyrights.
We will remove access to the work immediately and investigate your claim.

This work is downloaded from Delft University of Technology.

Journal of Nuclear Materials 610 (2025) 155800

Contents lists available at ScienceDirect

Journal of Nuclear Materials

journal homepage: www.elsevier.com/locate/jnucmat

Low-temperature sintering of (U,Pu)O_2 MOX in mild oxidative conditions

Jacobus Boshoven [a], Jean-François Vigier [a], Philipp Pöml [a], Abibatou Ndiaye [b], Bertrand Morel [c], Rudy J.M. Konings [a,d], Karin Popa [a,*], Marco Cologna [a,*]

[a] European Commission, Joint Research Centre (JRC), Karlsruhe, Germany
[b] ORANO Projects, MELOX, Les Tourettes, D138A, 30200, Chusclan, France
[c] ORANO Support, 92320 Chatillon, France
[d] Faculty of Applied Sciences, Radiation Science & Technology Department, Delft University of Technology, Mekelweg 15, Delft 2629JB, the Netherlands

ARTICLE INFO

Keywords:
MOX
Sintering
Nuclear fuel
Diffusion

ABSTRACT

We compare typical reductive sintering conditions for U, Pu mixed oxides (4 h at 1700 °C in Ar/6 % H_2 + 1200 ppm H_2O) with lower temperature and mildly oxidative conditions (2 h at 1200 °C in $CO/CO_2 = 1/9$) and report on the resulting microstructures and homogeneity. We show that lower temperature and mildly oxidative conditions, without cover gas change, can give close-to stoichiometric, crack-free MOX pellets with a relative density of ~ 95 %, and we propose ways to improve the homogenisations of PuO_2 and UO_2 and increase the grain size.

1. Introduction

Uranium-plutonium mixed oxide (MOX) pellets are currently used as fuel in several nuclear reactors, as a way to reutilise plutonium produced during commercial operation [1,2]. They are also the reference fuel for most European fast neutron reactor demonstrators and prototypes [3]. Like UO_2, MOX fuel is manufactured by ceramic powder technologies, involving three steps, (i) powder production, (ii) forming of green pellets and (iii) sintering. This last step is particularly energivorous, as it requires reaching temperatures in the order of 1700 °C over several hours. Hydrogen and optionally traces of water are used in the cover gas to avoid phase transformations and to set the final oxygen to metal ratio to the desired values, typically between 1.97 and 2.00. A reduction of the sintering temperature could increase the production sustainability, not only by decreasing the energy consumption, as well as reducing the cost and increasing the durability of the furnaces. This may be achieved by tackling the main variables affecting the sintering rate (Fig. 1): (i) reducing the powder particle size and distribution [4] (ii) applying external driving forces, as done in pressure assisted sintering techniques [5], or (iii) increasing the diffusion coefficient of the slowest (rate--limiting) species (in fluorite-type oxides, the diffusivity of the cation in the face-centred cubic sublattice is much lower than that of oxygen in the simple cubic sublattice [6]).

This last approach is particularly appealing for UO_2 and MOX, as the metal self-diffusion coefficient (D) increases by orders of magnitude when increasing the oxygen stoichiometry above 2 - a relationship of $D_U \propto X^2$ was suggested for UO_{2+x} [7]. The extent of hyper-stoichiometry can be conveniently set by fixing the oxygen partial pressure of the processing gas during sintering, for example using appropriate mixtures of CO, CO_2, H_2 or H_2O [8].

This approach has been shown to decrease the sintering temperature from ~1700 °C to ~1100 °C and reduce significantly the production time. It is known as *low temperature sintering* (LTS), [9–11], *oxidative sintering* [12], or *NUKUSI* process (from the German Niedrigtemperatur-Kurzzeit-Sintern, translatable as "low-temperature, short-time sintering"), and used by Kraftwerk Union AG to produce 50 tons of UO_2 pellets for irradiation [12–14].

One of the drawbacks of the oxidative sintering is the need to change the atmosphere during processing, to reduce hyperstoichiometric UO_{2+x} to $UO_{2.00}$ [15]. Another peculiarity is the need to control the solarisation phenomenon - a form of growth of grains and closed pores and concomitant de-sintering, or de-densification [16], which can be either seen as a drawback, or conveniently used to tailor the density, closed porosity, and grain size distribution [12,17].

The low-temperature hyperstoichiometric sintering of MOX is less reported in the open literature than UO_2. Kutty et al. performed sintering studies by dilatometry of UO_2, UO_2 –20 % PuO_2, UO_2 –50 % PuO_2, UO_2 –76 % PuO_2 and PuO_2, showing that an oxidising atmosphere lowers the onset temperature for densification for MOX [18,19], while pure PuO_2 sinters better in Ar –8 % H_2 compared to CO_2 [20]. Recently, Miranda

* Corresponding authors.
E-mail address: marco.cologna@ec.europa.eu (M. Cologna).

https://doi.org/10.1016/j.jnucmat.2025.155800
Received 21 February 2025; Received in revised form 27 March 2025; Accepted 31 March 2025
Available online 1 April 2025
0022-3115/© 2025 The Authors. Published by Elsevier B.V. This is an open access article under the CC BY license (http://creativecommons.org/licenses/by/4.0/).

et al. [21]. performed a dilatometry study of $U_{0.89}Pu_{0.11}O_{2+x}$ MOX fuel in a well-defined oxygen partial pressure (Ar + 4 vpm O_2), and observed significant swelling above 1200 °C, with development of the typical solarised microstructures. The pressure of the gas trapped in the closed porosity is responsible for swelling, which counteracts the intrinsic sintering pressure. Miranda et al. convincingly identified this gas as the oxygen released during reduction of U and Pu oxides at higher temperatures, and not CO or CO_2 as previously believed [21]. Barzati et al. [22], studied the solid solution formation in the $U_{0.7}Pu_{0.3}O_{2+x}$ system at 1400 °C, found no reaction in He + 5 % H_2, and complete interdiffusion by increasing the oxygen partial pressure with water vapour. Using an excessively high oxygen partial pressure, gave low-quality pellets, because of solarisation and fracturing induced by phase changes.

Here we compare conventional sintering conditions for MOX (1700 °C in $Ar/H_2/H_2O$) with low-temperature (1200 °C), mildly oxidative conditions, and we report on the resulting microstructures and homogeneity. We show that lower temperature and mildly oxidative conditions, in CO/CO_2 = 1/9 without gas change, can give close-to stoichiometric, crack-free MOX pellets with high density, and we propose ways to improve the homogenisations of PuO_2 and UO_2 and increase the grain size.

2. Experimental

2.1. Sample preparation

The starting uranium oxide powder was a commercial powder (Cogema TU2) with an average stoichiometry of $UO_{2.12}$, granules in the order of 10 μm and primary particles in the order of 0.2 –0.3 μm. The plutonium oxide powder was $PuO_{2.00}$ produced from oxalate precipitation, thus presenting the typical platelet morphology of several μm length. A more detailed characterisation is given elsewhere [4].

The feed powder mixture with a target composition of 0.11 Pu/(Pu + *U*) was prepared by dry vibratory milling (Retsch MM301) by adding the powders (2.438 g PuO_2 and 19.692 g UO_2) and three 12 mm diameter zirconia balls to a 25 ml zirconia jar. The mixture was milled for 2.5 h at a frequency of 15 s^{-1} and 5 h at 20 s^{-1} with 4 cooling breaks in total.

The density of the powders was measured by pouring the powder in a 10 ml glass cylinder and measuring the weight and the volume of the "as poured" powder (bulk density) and after gently shaking and tapping the cylinder until the powder volume showed no further decrease (tap density).

The milled powder without any additives was pressed at 405 MPa in a bi-directional press (Lauffer VIUG16), in 7.2 mm diameter dies lubricated on the surface with zinc stearate, into several green pellets (h ~ 5.8 mm) and disks (h ~ 1.4 mm) with a relative density of 69.7 % (the theoretical density (TD) of the solid mixture was estimated at 11.01 $g{\cdot}cm^{-3}$).

The green bodies were sintered either in "reductive" or "oxidising atmosphere". The reductive sintering took place in a metallic furnace (Degussa VSL10/18) on a molybdenum tray, in flowing Ar + 6 % H_2 moisturized with 1200 ppm of water vapour. The moisturized gas was used only from 600 °C, to prevent possible oxidation of the molybdenum at high oxygen potential at lower temperatures. Heating and cooling rates were 200 °C/h. The sintering schedule was as follows: heating to 600 °C in Ar/H_2, addition of 1200 ppm H_2O and dwell for 2 h, heating to 1700 °C and dwell for 4 h, cooling to 600 °C, switching-off of moisture and 1 h dwell in dry Ar/H_2, cooling to room temperature.

Oxidative sintering was performed in an alumina tubular furnace (AET) on an alumina tray at 1200 °C for 2 h. Heating and cooling rates were 200 °C/min. The furnace was flushed with a 10/90 mixture of carbon monoxide and carbon dioxide (BASI) with following specifications: 9.934 vol % CO (99.9 % purity) and rest CO_2 (99.995 purity). After the oxidative sintering, some samples were re-annealed in the same gas as the reductive sintering (Ar + 6 % H_2 + 1200 ppm H_2O) at 600 °C for 2 h.

Green and sintered densities were measured geometrically, by measuring the weights on a balance (KERN PCB350) and the diameter and the height with a micrometer (Mitutoyo QuickMike), and with the Archimedes's method for the sintered samples only, using a Sartorius BP211D balance equipped with a hydrostatic density kit.

2.2. Characterization techniques

The samples were analysed with a Bruker D8 X-ray diffractometer in a Bragg–Brentano configuration with a curved Ge monochromator (1,1,1), a copper tube (40 kV, 40 mA), equipped with a LinxEye position sensitive detector. Fragments of sintered pellets were pulverised in a mortar and deposited on a silicon wafer with a few drops of isopropanol. Profile refinement and structural analyses were performed with the JANA 2006 software suite.

The O/M ratio was measured by thermogravimetric analysis (TGA) with an oxidation/reduction procedure, adapted from ASTM C1817–16 to heating in a thermobalance. A fragment from the sintered pellets weighting > 100 mg was placed in a pre-treated Al_2O_3 crucible and inserted in a TGA (Netzsch 449C) and subjected to the following schedule, with a gas flow of 60 ml/min: (i) heating in Ar at 10 °C/min to 900 °C, and 10 min isotherm, (ii) switching gas to air for one minute, (iii) switching again to argon for 10 min, (iv) switching to Ar/H_2 and keeping the temperature at 900 °C for 160 min, and finally cooling.

The Pu/(*U*+Pu) ratio of the sintered pellets was measured by IDMS (Isotopic Dilution Thermal Ionisation Mass Spectrometry) using a Triton from Thermo Fisher Scientific GmbH.

Scanning Electron Microscopy (SEM) images were obtained with a Philips/FEI™ XL40 SEM placed inside a glovebox. The grain size was measured on the "as sintered" surface with the line intercept method without correction factor, using 4 SEM images and a minimum of 8 lines.

Electron micro probe analyzer (EPMA) measurements were carried out using a shielded Cameca SX100R equipped with four WDS spectrometers. The device was operated at an acceleration potential of 25 kV and a beam current of 100 nA. The 512×512 μm maps are stage scan maps with a pixel dwelling time of 100 ms and 256×256 pixels. The

$$\dot{\rho} = \frac{f(\rho, geom)}{T} \cdot \frac{1}{d^m} \cdot D_0 e^{-\frac{Q_a}{RT}} \cdot \left(g\frac{\gamma_{SV}}{\lambda} + P_E \right)$$

Densification rate — Particle size — Diffusivity — Driving force

Fig. 1. The variables affecting the sintering rate, where f is a function of the density (ρ) and of the geometry, and includes mechanism-dependent constant terms, *d* is the particle size, *m* is a mechanism-dependent exponent ($m = 2$ for volume diffusion-controlled sintering, and $m = 3$ for grain boundary diffusion-controlled sintering), D_0 is the pre-exponential factor of the diffusion coefficient of the slowest species along the fastest path, with activation energy Q_a. The last term represents the driving force, which is given by the sum of the effective external pressure, P_E (which is 0 for free sintering) and the intrinsic sintering pressure ($g\ \gamma_{SV}/\lambda$), where *g* is a geometric term, λ a geometric scale of the microstructure, typically *d* or the pore radius.

100×100 μm maps are beam scan maps with a pixel dwelling time of 500 ms and 256×256 pixels. No off-peak background correction maps were recorded for the 512×512 μm maps; the 100×100 μm maps were background corrected using off peak maps with a dwelling time of 100 ms. For the analysis of Pu and U a QTZ diffraction crystal was used, while for Zr a PET crystal was used. Oxygen was calculated by stoichiometry. As reference materials PuO_2, UO_2 and ZrO_2 were used. As X-ray lines U Mα, Pu Mβ and Zr Lα were used. The Pu Mβ intensity was corrected for an interference with the U M3-N4 line. As matrix correction algorithm the "PAP" procedure was used, and the data were processed with the Probe for EPMA software package.

3. Results

The bulk and tapped densities in $g \cdot cm^{-3}$ were 2.11 and 2.52 for UO_2, 2.54 and 3.57 for PuO_2, 2.11 and 2.65 for MOX before milling, and 2.65 and 3.81 for MOX after milling, respectively. Milling thus increases significantly both the tap and bulk density, yielding better flowing powder. The powder mixture after milling consisted of granules of different sizes, from a few tents to a few hundreds of micrometres. An example is given in Fig. 2, where the fine sub-micrometre particles are UO_2 and some platelets of several micrometres in size, typical of PuO_2 powders obtained from oxalate precipitation, are still visible.

The geometrical and Archimedes density after sintering is given in Table 1.

X-ray diffraction (XRD) analysis was performed on samples sintered in three different conditions: (i) sintered at 1700 °C in Ar + 6 % H_2 + 1200 ppm H_2O, (ii) at 1200 °C in CO/CO_2, and (iii) at 1200 °C in CO/CO_2 and annealed at 600 °C in Ar + 6 % H_2 + 1200 ppm H_2O. The diffractograms are given in Fig. 3. The MOX sintered at 1700 °C in a reducing atmosphere shows a clear peak separation at high angles (see insets in Fig. 3), thus the solid solution of PuO_2 and UO_2 has not completely formed. The average composition of the two phases can be estimated by using the Vegard's law, assuming an oxygen to metal ratio of 2 and lattice parameters $a_0(UO_2) = 5.4715$ Å and $a_0(PuO_2) = 5.397$ Å (Table 2). Both phases, $(U_{0.94}Pu_{0.06})O_2$ and $(U_{0.84}Pu_{0.16})O_2$, are rich in U and are present in similar quantities. Due to their similar lattice parameters, diffraction peaks are strongly overlapping, and the presence of the two phases is clearly distinguished on the diffractogram only at high angles where the separation is stronger. Conversely, the samples sintered at 1200 °C in CO/CO_2, with or without post-annealing, show small but clearly distinguishable peaks of a second phase already at low angles (inset of Fig. 3). Here we will discuss only one of the two samples, as the one after annealing shows no significant difference. The two phases have very distinct lattice parameters, and consist of a U-rich phase $(U_{0.94}Pu_{0.06})$ and a Pu-rich one $(U_{0.03}Pu_{0.97}O_2)$. This second phase, with composition very close to the original PuO_2 powder, is present in concentrations of <4 %, a significant reduction compared to the original 11 %. The average composition of the three MOX samples, when calculated from the weighted average of the lattice parameters of their constituent phases and their respective concentrations, is $U_{0.90}Pu_{0.10}O_2$, very close to the nominal composition. In this case, due to the large difference of lattice parameters, the diffraction peaks do not overlap, even at the low angle of the diffractogram where the two phases are clearly identified. However, due to the very low concentration of Pu-rich phase, the diffraction peaks become difficult to distinguish at high angle where the intensity is lower.

The Pu/(*U*+Pu) ratio of the sintered pellets was confirmed by IDMS to be the nominal 11 %. The O/M ratio, as calculated from the TGA experiments was 2.01 ± 0.01 for the reductive sintering, and 2.00 ± 0.01 for the other samples. Within the measurement error, all samples can be considered at the same O/M, close to stoichiometry. The

Table 1
Geometrical and Archimedes density, in percentage of theoretical density. The reported average and standard deviation are on a population of four samples for each conditions.

Sintering conditions	Geom. Density [%TD]	Arch. Density [%TD]
$Ar/H_2 + H_2O$ at 1700 °C	97.6 ± 1.3	98.1 ± 0.1
CO/CO_2 at 1200 °C	95.9 ± 2.2	95.1 ± 0.8

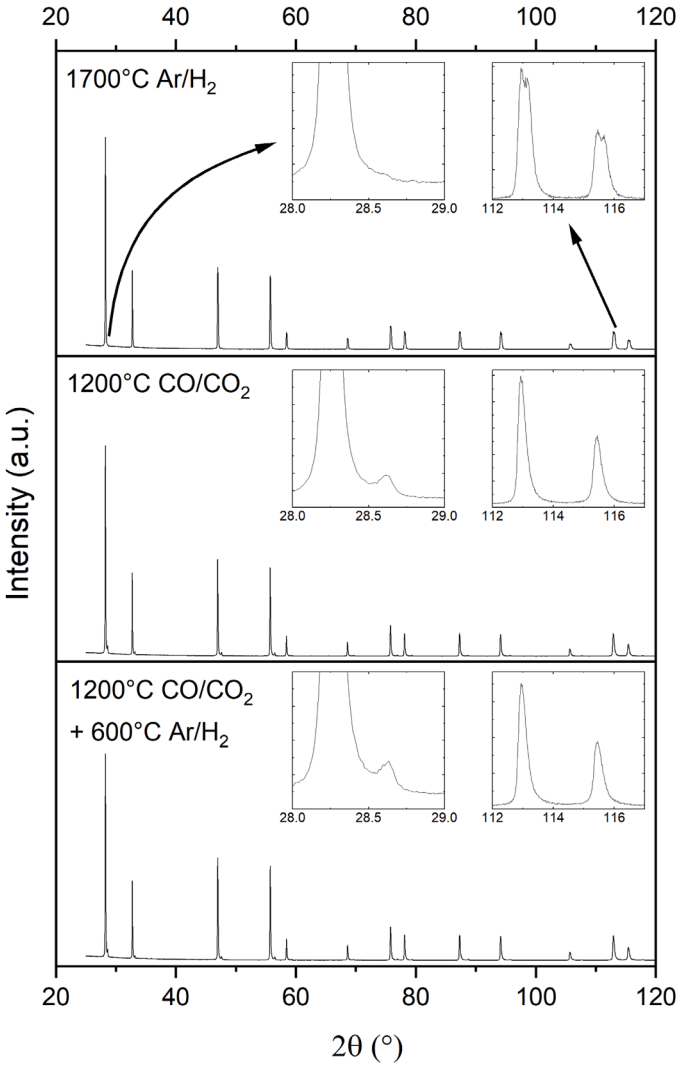


Fig. 3. XRD diffractograms of sintered MOX Pellets.

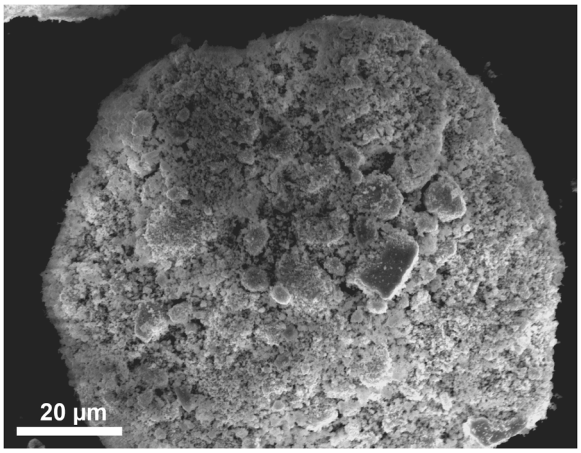


Fig. 2. SEM of a typical granule of the milled MOX powder.

Table 2
Cell parameter a_0 from XRD analysis and calculated phase amounts and compositions using the Vegard's law between $UO_{2.00}$ and $PuO_{2.00}$.

Sintering conditions	Phase	Amount	a_0 (Å)	Composition
1700 °C in $Ar/H_2 + H_2O$	1	58.2 %	5.4670 (2)	$(U_{0.94}Pu_{0.06})O_2$
	2	41.8 %	5.4594 (2)	$(U_{0.84}Pu_{0.16})O_2$
	weighted av.		5.4638	$(U_{0.90}Pu_{0.10})O_2$
1200 °C in CO/CO_2	1	96.3 %	5.4668 (2)	$(U_{0.94}Pu_{0.06})O_2$
	2	3.7 %	5.3989 (6)	$(U_{0.03}Pu_{0.97})O_2$
	weighted av.		5.4644	$(U_{0.90}Pu_{0.10})O_2$
1200 °C in CO/CO_2 and 600 °C in $Ar/H_2 + H_2O$	1	96.7 %	5.4664 (2)	$(U_{0.93}Pu_{0.07})O_2$
	2	3.3 %	5.3986 (6)	$(U_{0.02}Pu_{0.98})O_2$
	weighted av.		5.4641	$(U_{0.90}Pu_{0.10})O_2$

additional reduction step of the oxidative sintered pellets did not change the oxygen content, as can be concluded also from the unchanged lattice parameter.

Microstructures of the pellets are given in Fig. 4 ("as sintered" free surface) and Fig. 5 (fracture surface). Since the low-temperature annealing at 600 °C did not change the microstructure, only one sample is reported for the oxidative sintering. The mean grain size evaluated on the surface is 2.3 ± 0.5 μm and 1.3 ± 0.2 μm, for the reductive and oxidative sintered samples, respectively. The pellets sintered in reducing gas atmosphere show less porosity (Fig. 5, left), but the pore size is larger than the pellets sintered in oxidizing gas atmosphere (Fig. 5, right).

The U and Pu distribution as measured by EMPA is shown in Fig. 6. Both samples show spots with higher concentration of Pu. Such spots, with sizes below 10 μm, are homogenously distributed within the microstructure. Clearly, the inter-diffusion for the sample sintered at 1200 °C in oxidative conditions has been less effective, and more spots rich in Pu are visible.

4.4. Discussion

When sintering is conducted in a buffer gas, such as a CO and CO_2 mixture at high temperature, the following equilibrium is rapidly reached, e.g. [23]:

$$CO(g) + \frac{1}{2}O_2(g) = CO_2(g) \quad (1)$$

The oxygen partial pressure in the gas, for a fixed CO to CO_2 ratio in the inlet gas, can be determined from the equilibrium constant, K_C:

$$K_C = \frac{p_{CO_2}}{p_{CO}\left(p_{O_2}\right)^{1/2}} \quad (2)$$

and

$$K_C = e^{-\left(\frac{\Delta G_c^0}{RT}\right)} \quad (3)$$

Where ΔG_c^0 is the standard-state Gibbs-energy change of the reaction in Eq. (1), and thus:

$$\Delta G_c^0 = \Delta H_c^0 - T\Delta S_c^0 \quad (4)$$

Where T is the temperature, ΔH_c^0 the standard enthalpy change (−282.4 kJ/mol) and ΔS_c^0 the standard entropy change (−86.8 J/(mol·K)) [23]). The oxygen potential of the gas mixture can be calculated from the oxygen partial pressure as:

$$\Delta G_{O_2} = RT\, ln\, p_{O_2} \quad (5)$$

In a similar way, the oxygen partial pressure set by the water/hydrogen buffer gas, was calculated for the reaction

$$H_2(g) + \frac{1}{2}O_2(g) = H_2O(g) \quad (6)$$

with $\Delta H_c^0 = -246.44$ kJ/mol and $\Delta S_c^0 = -54.81$ J/(mol·K) [24].

The oxygen partial pressure and potential of the selected buffer gases are given in Fig. 7. The used atmosphere of $Ar/H_2/H_2O$ sets the oxygen potential at 1700 °C to - 405 kJ/mol, and at 600 °C to - 454 kJ/mol, while CO/CO_2 sets the oxygen potential at 1200 °C to - 255 kJ/mol and at 600 °C to - 381 kJ/mol.

The oxidative conditions chosen here are milder compared to other results reported in the literature. Miranda [21], sintered 11 % Pu-MOX in Ar + 4 vpm O_2 up to 1540 °C, which corresponds to an oxygen potential of −187 kJ/mol at 1540 °C and −90 kJ/mol at 600 °C. In such conditions, the experimentally measured O/M ratio achieved a maximum of 2.31 and reached 2.22 during cooling. The density of the pellets reached a maximum at 1200 °C, after which significant swelling occurred. Barzati [22], sintered 30 % Pu-MOX in Ar + 100 ppm O_2 and Ar + 500 ppm O_2, and Kutty [18] used CO_2. Such conditions are strongly oxidative and induce a large deviation from stoichiometry.

During the mild oxidative conditions reported here, the O/M of 11 % Pu –MOX at 1200 °C is kept at values higher than 2.00, but below 2.01, e.g. from Fig. 1 in Ref. [21]. Also during cooling, at 600 °C, either in CO/CO_2 or during the optional annealing in $Ar/H_2/H_2O$, the samples are expected to remain very slightly hyperstoichiometric ($2.00 < O/M < 2.01$). On the other hand, sintering in conventional conditions in $Ar/H_2/H_2O$, sets an oxygen partial pressure giving a slightly hypostoichiometric composition (O/M ~ 1.99). During cooling, the samples

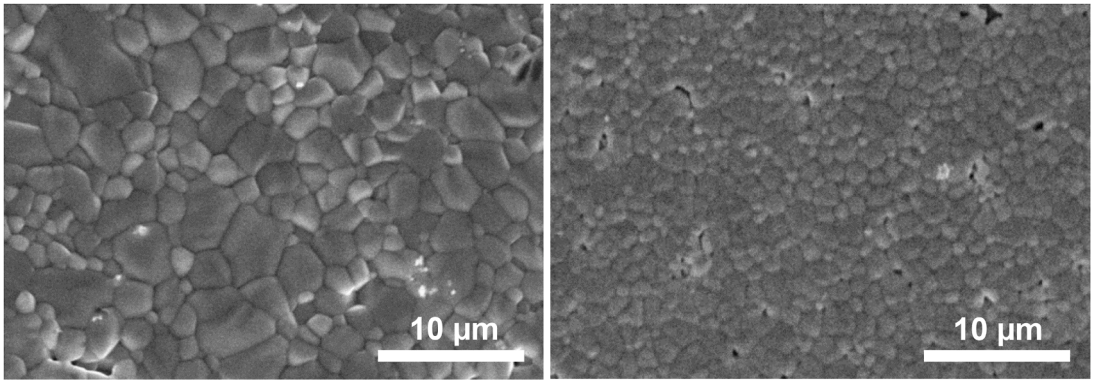


Fig. 4. SEM of the free surface of samples sintered at 1700 °C in Ar/H_2 (left) and at 1200 °C in CO/CO_2 (right).

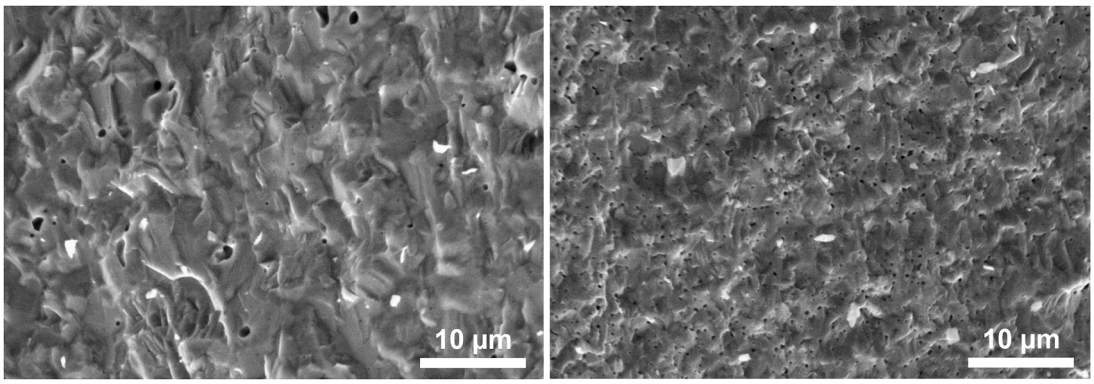


Fig. 5. SEM of the fracture surface of samples sintered at 1700 °C in Ar/H_2 (left) and at 1200 °C in CO/CO_2 (right).

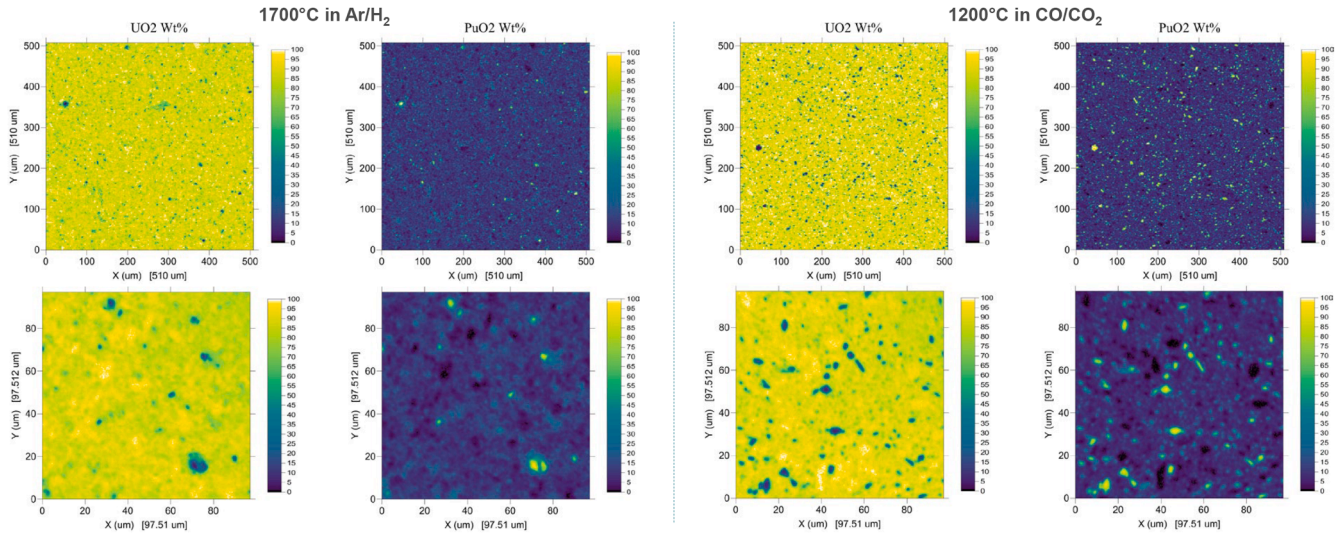


Fig. 6. Distribution of UO_2 and PuO_2 measured by EPMA on polished cross sections of samples sintered at 1700 °C in Ar/H_2 (left side) and at 1200 °C in CO/CO_2 (right side). Images in the bottom row are at a higher magnification (5x) than in the top row.

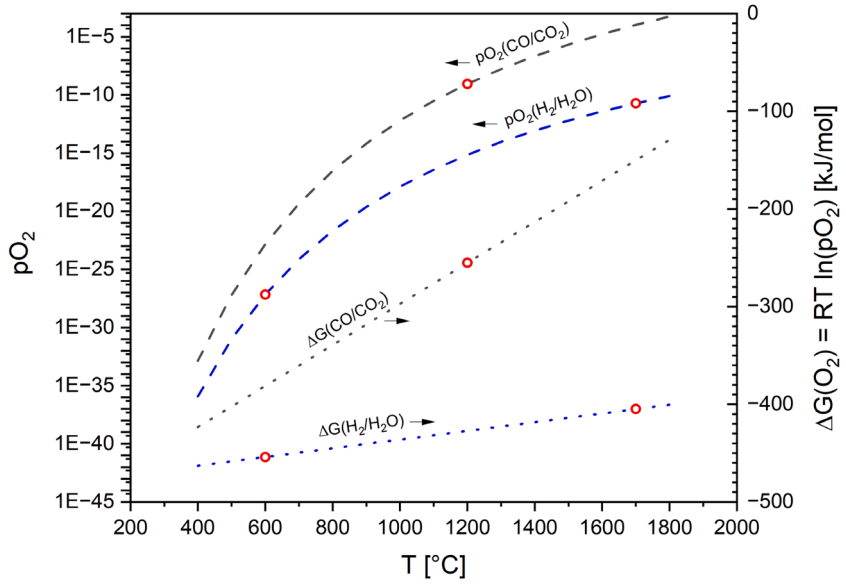


Fig. 7. Oxygen partial pressure and potential as a function of the temperature for the selected buffer couples: CO/CO2 = 1/9 (black curves), and H_2/H_2O= 0.06/0.0012 (blue curves). The red dots specify the selected sintering and annealing conditions.

are expected to become slightly hyperstoichiometric, although with O/M very close to 2.00. These differences are not captured by the analysis methods used here, which have an estimated error of ± 0.01 O/M, so that we can only observe that, the samples are close-to stoichiometric for any conditions.

The low-temperature oxidative conditions used here are sufficient to achieve crack-free pellets with high relative density (~ 95 %) and a microstructure with closed porosity. However, the density, grain size, and degree of solid solution formation from UO_2 and PuO_2 end members are lower than those of the samples sintered for 4 h at 1700 °C.

A typical and effective solution to increase such properties would be to increase the sintering temperature (the diffusion coefficients increase strongly with the temperature, following the Arrhenius law). However, at temperatures > 1200 °C in oxidative conditions, de-sintering may start to occur [21], although, if the reason for solarisation is the oxygen gas released during the reduction of U and Pu oxides at higher temperatures [21], solarisation may be less of a problem for the milder oxidative conditions studied here ($2.00 < O/M < 2.01$).

An alternative would be to increase the dwell time at 1200 °C. We can estimate the time that would be needed to achieve the desired grain size as follows: in isothermal conditions, the average grain size G grows with the time t as $G^n - G_0^n = kt$, with k the grain growth constant, n the grain growth exponent, and G_0 the initial grain size at $t = 0$; since $G >> G_0$ and assuming $n = 2$ (the typical value for dense ceramic oxides), the average grain size has a time dependency of the type $G \propto t^{1/2}$. Thus, increasing the isothermal dwell time at 1200 °C from 2 h to 8 h would double the grain size, allowing reaching a similar microstructure as the samples sintered for 4 h at 1700 °C in reducing conditions. Longer dwell times, would also be beneficial for the homogenisation of UO_2 and PuO_2. A high homogeneity in the U/Pu distribution is thought to give a better behaviour under reactor irradiation, by preventing the local formation of the high-burnup structure [25]. However, it is worth mentioning that increasing significantly the sintering duration would have a significant impact on the plant throughput.

Improvements in this aspect are also possible by a better homogenisation of the starting powder. The vibratory milling used here is not very efficient in terms of comminution (large particles of PuO_2 are still present after milling the mixed powder, Fig. 1), and planetary milling is expected to give better results.

The use of powders with smaller particle size could also bring a further improvement: it has been recently shown that highly homogeneous $U_{0.89}Pu_{0.11}O_2$ MOX with larger grain size is achieved in a conventional powder milling and reductive sintering process, only by replacing the typical ex-oxalate PuO_2 powder by nano-PuO_2 powders obtained by hydrothermal precipitation [4]. Combining the mild oxidative sintering conditions in CO/CO_2 and nano-PuO_2, could give larger grain size and better homogeneity already at 1200 °C.

5. Conclusions

Nuclear reactor UO_2 fuel pellets are typically obtained in a high-temperature energy-intensive sintering process, where H_2 gas is used to set reducing conditions. As an attempt to decrease the process energy and the cost and complexity of sintering furnaces, an alternative low-temperature oxidative sintering process for UO_2 was developed and reported in the literature in the last decades. However, concerning (U, Pu)O_2 MOX fuel, less information is available in the open literature.

The results reported in this paper, show that the use of low-temperature, mildly oxidative conditions (2 h at 1200 °C in CO/CO_2 = 1/9) is an effective way to sinter (U,Pu)O_2 MOX pellets to high density and closed porosity. The obtained MOX pellets are crack-free and close to stoichiometric. The grain size and the density are still lower compared to the same samples sintered for longer time in typical reducing conditions (4 h at 1700 °C in Ar/H_2), as well as the degree of homogenisation of U and Pu. Optimisation of the process is expected to further improve the microstructural features. This may be achieved by increasing the dwell time at 1200 °C, improving the homogenisation of the powder mixture, or using smaller size PuO_2 as starting powders.

CRediT authorship contribution statement

Jacobus Boshoven: Writing – review & editing, Writing – original draft, Investigation. **Jean-François Vigier:** Writing – review & editing, Investigation, Formal analysis. **Philipp Pöml:** Writing – review & editing, Investigation. **Abibatou Ndiaye:** Writing – review & editing, Formal analysis, Conceptualization. **Bertrand Morel:** Writing – review & editing, Funding acquisition, Conceptualization. **Rudy J.M. Konings:** Writing – review & editing, Supervision, Funding acquisition, Conceptualization. **Karin Popa:** Writing – review & editing, Writing – original draft, Supervision, Investigation. **Marco Cologna:** Writing – review & editing, Writing – original draft, Supervision, Formal analysis.

Declaration of competing interest

The authors declare that they have no known competing financial interests or personal relationships that could have appeared to influence the work reported in this article.

Acknowledgements

The work was partially conducted under a Third Party Work (TPW) contract 35733. We are grateful to the JRC Analytical Services for chemical analysis, to Herwin Hein for TGA measurements, to Daniel Bouëxière for XRD measurements, and Ramon Carlos Marquez for SEM.

Data availability

Data will be made available on request.

References

[1] F. La Lumia, L. Ramond, C. Pagnoux, P. Coste, F. Lebreton, J.R. Sevilla, G. Bernard-Granger, Dense and homogeneous MOX fuel pellets manufactured using the freeze granulation route, J. Amer. Ceram. Soc. (2020) 3020–3029.
[2] S. Fehér, T. Reiss, A. Wirth, MOX fuel effects on the isotope inventory in LWRs, Nucl. Eng. Des. 252 (2012) 201–208.
[3] L. Malerba, A. Al Mazouzi, M. Bertolus, M. Cologna, P. Efsing, A. Jianu, P. Kinnunen, K.-F. Nilsson, M. Rabung, M. Tarantino, Materials for sustainable nuclear energy:a European strategic research and innovation agenda for all reactor generations, Energies (2022) 1845.
[4] J. Boshoven, A. Ndiaye, B. Morel, M. Cologna, J.-F. Vigier, R.C. Marquez, R.J. M. Konings, K. Popa, Homogeneous $U_{0.89}Pu_{0.11}O_2$ mixed oxide by use of PuO_2 nanopowders, J. Nucl. Mater. (2025) under review.
[5] M. Cologna, 5.25 - Use of field assisted sintering for innovation in nuclear ceramics manufacturing. Comprehensive Nuclear Materials (Second Edition), 2020, pp. 811–839.
[6] K. Ando, Y. Oishi, Diffusion characteristics of actinide oxides, J. Nucl. Sci. Technol. (1983) 973–982.
[7] H. Matzke, Lattice disorder and metal self-diffusion in non-stoichiometric UO_2 and (U, Pu)O_2, J. Phys. Collo. (1973) C9–317. -C9-325.
[8] J. Williams, E. Barnes, R. Scott, A. Hall, Sintering of uranium oxides of composition UO_2 to U_3O_8 in various atmospheres, J. Nucl. Mater. (1959) 28–38.
[9] N. Fuhrman, L.D. Hower JR, R.B. Holden, Low-temperature sintering of uranium dioxide, J. Am. Ceram. Soc. (1963) 114–121.
[10] X.-D. Yang, J-C. Gao, Y. Wang, X. Chang, Low-temperature sintering process for UO_2 pellets in partially-oxidative atmosphere, Trans. Nonferr. Metals Soc. China (2008) 171–177.
[11] T.R.G. Kutty, P.V. Hegde, K.B. Khan, U. Basak, S.N. Pillai, A.K. Sengupta, G.C. Jain, S. Majumdar, H.S. Kamath, D.S.C. Purushotham, Densification behaviour of UO_2 in six different atmospheres, J. Nucl. Mater. (2002) 159–168.
[12] H. Assmann, W. Dorr, N. Peeks, Control of UO2 microstructure by oxidative sintering, J. Nucl. Mater. (1986) 1–6.
[13] IAEA-TECDOC-1686, Experiences and Trends of Manufacturing Technology of Advanced Nuclear Fuels, 2012.
[14] E. González-Robles, V. Metz, D.H. Wegen, M. Herm, D. Papaioannou, E. Bohnert, R. Gretter, N. Müller, R. Nasyrow, W. de Weerd, T. Wiss, B. Kienzler, Determination of fission gas release of spent nuclear fuel in puncturing test and in leaching experiments under anoxic conditions, J. Nucl. Mater. (2016) 67–75.
[15] D.G. Frost, P.A. Burr, E.G. Obbard, J. Veliscek-Carolan, Controlling low temperature sintering of UO_{2+x}, J. Nucl. Mater. (2024) 155269.

[16] I. Amato, R.L. Colombo, A.M. Protti, On a case of solarization during steam sintering of UO_2 pellets, J. Nucl. Mater. (1963) 271–272.
[17] W. Dörr, G. Maier, M. Peehs, Einstellung und charakterisierung der strukturgrössen von LWR-Brennstoff, J. Nucl. Mater. (1982) 61–67.
[18] T.R.G. Kutty, P.V. Hegde, K.B. Khan, S. Majumdar, D.S.C. Purushotham, Sintering studies on UO_2–PuO_2 pellets with varying PuO_2 content using dilatometry, J. Nucl. Mater. (2000) 54–65.
[19] T.R.G. Kutty, P.V. Hegde, R. Keswani, K.B. Khan, S. Majumdar, D.S. C. Purushotham, Densification behaviour of UO_2-50%PuO_2 pellets by dilatometry, J. Nucl. Mater. (1999) 10–19.
[20] T.R.G. Kutty, K.B. Khan, P.V. Hegde, A.K. Sengupta, S. Majumdar, D.S. C. Purushotham, Densification behaviour and sintering kinetics of PuO_2 pellets, J. Nucl. Mater. (2001) 120–128.
[21] G.C.C. Miranda, L. Ramond, F. Lebreton, P. Signoret, P. Martin, A. Ndiaye, T. Gervais, G. Bernard-Granger, MOX fuel sintering under oxidizing conditions: a comprehensive study of the solarisation phenomenon, J. Eur. Ceram. Soc. (2023) 6373–6385.
[22] S. Berzati, S. Vaudez, R.C. Belin, J. Léchelle, Y. Marc, J.-C. Richaud, J.-M. Heintz, Controlling the oxygen potential to improve the densification and the solid solution formation of uranium–plutonium mixed oxides, J. Nucl. Mater. (2014) 115–124.
[23] D.R. Olander, Fundamental Aspects of Nuclear Reactor Fuel Elements, US DoE, 1976, p. 149.
[24] M. Kato, K. Takeuchi, T. Uchida, T. Sunaoshi, K. Konashi, Oxygen potential of $(U_{0.88}Pu_{0.12})O_{2\pm x}$ and $(U_{0.7}Pu_{0.3})O_{2\pm x}$ at high temperatures of 1673-1873K, J. Nucl. Mater. 414 (2011) 120–125.
[25] M. Le Guellec, F. Lebreton, L. Ramond, A. Ndiaye, T. Gervais, G. Bernard-Granger, Sintering investigations of a UO_2-PuO_2 powder synthesized using the freeze-granulation route, Scripta materialia (2010) 190–195.